

RESEARCH

Open Access



Structural Performance of Ferrocement Hollow Shear Walls Subjected to Lateral and Compressive Axial Loads

Yousry B. Shaheen¹, Boshra A. Eltaly¹ , Samar Khairy² and Sabry Fayed^{3*}

Abstract

In this study, ten shear walls were experimentally tested to examine behaviour of ferrocement hollow shear walls subjected to axial and lateral loads. Ferrocement mortar (FM) was used to build eight walls, while normal concrete (NC) was used to build two controls. Walls were lateral reinforced using conventional stirrups, two layers of welded wire mesh (WWM), and expanded steel mesh (ESM). Two specimens lacked lateral reinforcement except for one transverse web in the center of the inner hole. Two symmetric groups of five walls each were created by dividing the walls. While the other group was loaded laterally, one group was loaded axially. In each group, the load–displacement relationship, maximum load and associated displacement, stiffness, ductility, and failure mechanism of FM and NC walls were compared. The results showed that FM walls provided with ESM and WWM had ultimate axial loads that were, respectively, 36% and 19% higher than NC control walls. Ultimate lateral loads and related ultimate drifts of FM walls reinforced with two layers of WWM and ESM were, respectively, 68% and 39%, 96% and 43.5%, larger than control NC wall. For lateral loads greater than those applied to the NC control wall, stiffness increase ratios for FM walls ranged from 2.5% to 89.5%, and for axial loads, they ranged from 20% to 150.5%. The ductility of FM walls increased when compared to NC walls by 58.5% and 158.8% for axial and lateral loading, respectively, when two layers of WWM were utilized to lateral reinforce FM walls. When two layers of ESM were applied to laterally reinforce FM walls in comparison to an NC wall, this increased the walls' ductility under axial and lateral loads by 110.5% and 214.7%, respectively.

Keywords Ferrocement mortar, Shear walls, Steel mesh, Lateral loading, Ultimate load, Ductility

1 Introduction

Because they have a high resistance to lateral seismic stresses, shear walls are vertical structural components of systems that resist horizontal forces and are found

in earthquake zones. The building is safer and sturdier thanks to the use of these walls. Studying the structural reaction and their systems in multi-story structures would, therefore, be highly intriguing. Shear walls need to be sufficiently ductile to prevent brittle collapse in the presence of powerful lateral earthquake forces (Greifenhagen and Lestuzzi 2005; Orakcal et al. 2009).

Various types of reinforcement for shear walls have been studied by numerous researchers. Oh et al. (2002) investigated the impact of boundary zone reinforcement details on the behaviour of 2.0 aspect ratio structural walls. Slender shear walls were tested by Hube et al. (2014). According to their findings, the tested walls broke in a compressive failure manner and reserved

Journal information: ISSN 1976-0485 / eISSN 2234-1315.

*Correspondence:

Sabry Fayed

sabry_fayed@eng.kfs.edu.eg

¹ Department of Civil Engineering, Menoufia University, Shebin El Koum, Egypt

² Department of Civil Engineering, Higher Institute of Engineering and Technology, Kafr El Sheikh, Egypt

³ Department of Civil Engineering, Faculty of Engineering, Kafr El-Sheikh University, Kafr El-Sheikh, Egypt

their predicted flexural capability. Christidis and Trezos (2017) conducted assessment research on shear walls that were not designed in accordance with Eurocode and came to the conclusion that the walls' nonconformance to contemporary standards had little to no impact on the evaluated specimens' ability to bear weight. With the use of the experimental data, Christidis and Karagiannaki (2021) computed the shear and flexure displacement components for four cantilever medium-rise poorly reinforced concrete shear walls. On RC walls, Altheeb (2016) carried out an experimental investigation. In contrast to other seismically active regions like Turkey and Greece, the specimens used in this study only had one layer of vertical and horizontal steel. In New Zealand's moderate earthquake zones, RC shear walls employed in high-rise buildings were put to the test by Lu et al. (2017). Although the results indicated that one or two base-level cracks were responsible for the behaviour of the samples and that they limited the shear walls' ability to drift, bar slip was not studied and measured individually. The effects of large-scale wall behaviour without particular boundary features were examined by Motter et al. (2018), who also suggested modifying the limiting parameters used in current codes.

Recent years have seen the development of new uses for ferrocement, including low-cost housing structures. These applications, though, are still in their infancy. Ferrocement is a material that has been created with the environment in mind. A type of thin wall reinforced concrete structure known as a ferrocement uses layers of mesh with very small wire diameter that are positioned closely together to reinforce hydraulic cement. The mesh could be created from metal or any appropriate material. The openness and tightness of the reinforcing system it is intended to envelop should be compatible with the fineness of the mortar matrix and its composition. Discontinuous fibres could be present in the matrix (ACI, 1993; Eltehawy, 2009; Gaba & Singh, 2008; Naaman, 2000; Wafa & Fukuzawa, 2010; Wang et al., 2004). Due to its advanced properties, such as its environmental friendliness, tensile strength (Greepala & Nimityongskul, 2006; Sasiekalaa & Malathy, 2012), flexibility, fine cracking, impermeability, ductility, toughness, fire resistance, water tightness, crack resistance, lightness, durability, cost, time, and construction technology, ferrocement has a very wide range of applications (Committee, 1997). Many researches have studied the effectiveness of ferrocement subjected to compression load (Mansur & Paramasivam, 1990; Shaheen et al., 2016; Xiong et al., 2011).

The use of steel meshes to strengthen the structural members made of ferrocement was investigated. Research on lateral reinforcement for square short RC columns using a single expanded metal mesh (EMM)

layer combined, in a practical manner, with various volumetric ratios of ties was presented by El-Kholy and Dahish (2016). The strength and ductility of the confined columns have improved noticeably with the suggested lateral reinforcement. Additionally, by adding the EMM layer, it may be possible to significantly lower the volumetric ratio of the ties without lowering the ultimate load. Shaheen et al. (2017)'s investigation into the behaviour of reinforced composite concrete columns included varied ratios of metallic and nonmetallic mesh reinforcement. The findings demonstrated that novel reinforced concrete columns with high strength, crack resistance, and high ductility properties could be made using cutting-edge composite materials. Numerous studies (Ganesan et al., 2011; Kaish et al., 2013; Kaushik & Singh, 1999; Kondraivendhan & Pradhan, 2009; Li et al., 2018; Ravichandran & Jeyasehar, 2012; Soman & Mohan, 2018; Xiong et al., 2011) focused on the reinforcement of columns using layers of ferrocement concrete and steel mesh, and it was found to be an innovative way to increase column capacity.

Since the ferrocement has superior mechanical properties and also the steel meshes improve the capacity of the structural elements, so that it is important to study the behavior of steel mesh-ferrocement shear wall composite. It is worth noting that the behavior of this element has not been studied before. As a result, the objective of the current paper is to examine the behavior of ferrocement shear wall strengthened with webs and subjected to axial and lateral loads. Ten walls with different volume fractions of steel reinforcement (stirrups, expanded steel mesh and welded wire mesh) were tested up to failure.

2 Research Significance

Because they have a high resistance to lateral seismic stresses, shear walls are vertical structural components of systems that resist horizontal forces and are found in earthquake zones. The building is safer and sturdier thanks to the usage of these walls. Shear walls give buildings a great deal of stiffness and strength, which effectively lessens lateral displacement of the structure and, as a result, lessens structural damage. Ferrocement mortar provides higher mechanical and fresh qualities, cracking control, maximum capacity, ductility, etc. in contrast to conventional concrete. It can be used to reinforce ferrocement mortar, which has the benefit of reducing the number of cracks, by encircling the concrete core of the shear wall with steel meshes. Additionally, steel meshes rather than conventional stirrups are utilized to laterally strengthen the wall to significantly improve the transverse confinement and hence boost the wall capacity. Prior research on the structural performance of cement shear walls exposed to lateral loads was lacking. All huge buildings requiring different construction

Table 1 Grading of sand and dolomite used

Particle size (mm)	Course					Fine					
	12	9.5	4.75	2.5	1.25	4.75	2.83	1.41	0.707	0.354	0.177
Pass (%)	97.1	88.4	13.8	3.2	1.6	97.7	89.7	67.5	49	3.8	1.6

Table 2 Proportions of NC mix

Component	Portland cement	Fine aggregate (sand)	Coarse aggregate (dolomite)	Water
Weight (kg/m ³)	350	665	1330	140

methods and heavy weights must have a substantial portion of walls in their plans. As a result, this study aims to comprehend how holing the wall core impacts ferrocement walls’ behaviour. The primary factors are the type of concrete (normal concrete and ferrocement mortar), the lateral shear reinforcement (discontinued stirrups and steel meshes), the lateral web within the inner hole, and the type of loading (axial and lateral).

3 Experimental Program

3.1 Materials

3.1.1 Concrete

3.1.1.1 Normal Concrete (NC) In this experiment, control shear wall specimens were cast using a common normal concrete (NC) mix with a compressive strength of 35 MPa. Sand, dolomite that has been crushed, water, and regular Portland cement are combined to form the NC mix. The employed cement has a grade of 42.5 and complies with Portland cement type I. In the current experiment, natural siliceous sand with a fineness modulus of 2.91, specific gravity of 2.51, and absorption of 0.50% was used. Crushed dolomite with a specific gravity of 2.4, a fineness modulus of 4.9, and an absorption of 1.50% was employed as the coarse aggregate. Sand and dolomite grading is depicted in Table 1. The maximum nominal aggregate sizes for sand and crushed dolomite are 4.75 mm and 12 mm, respectively. The proportions of the NC mix are stated in Table 2. Three cubes (150 mm on each side) and cylinders (150×300 mm) were taken from the NC mix during the casting of NC specimens to measure the compressive and splitting tensile strengths.

NC has compressive and cracking tensile strengths of 37.5 and 2.95 MPa after 28 days.

3.1.1.2 Ferrocement Mortar (FM) Table 3 lists the proportions of the ferrocement mortar (FM) mix. The basic components of FM mix are silica fume, polypropylene (PP) fibre, regular Portland cement, water, sand, and superplasticizers. To reach the desired compressive strength of 35 MPa, the amount of each element in FC mix is determined in accordance with ACI 549.1R-93 (1997).

It is generally known that this FM mix contains a substantial amount of cement and is devoid of coarse aggregate. Condensed silica fume in powder form with a light grey hue was used in place of some of the cement to make a high-strength mortar. It was used to substitute silica fume for 10% of the cement’s weight. Fibres without reprocessed hydrocarbon components that are specifically crafted to the optimal gradation used as secondary reinforcement in concrete. A minimum of 0.9 kg per cubic meter must be applied. Typically, fibres are used to stop cracking caused by thermal expansion and contraction as well as drying shrinkage. It was also used to add fibres to concrete, which increased the concrete’s toughness and residual strength, decreased concrete’s permeability, increased impact strength, raised shatter resistance, and improved abrasion resistance. To keep the threads from sticking to one another, polypropylene (PP) fibre was employed in this project and gradually added to the FM mix (agglomeration). Fig. 1 displays the PP fibre in use. PP fibre has a diameter and length of 0.012 and 18 mm, respectively, according to the manufacturer. As a superplasticizer, a high-range water reducer (type A and F) is used (Data sheet of Sika VisConcrete 3425 2024). To produce high-quality concrete and give the concrete mix the necessary workability, superplasticizers are used. The admixture used is a brown liquid with a density of 1.18 kg/liter at room temperature. The weight of the superplasticizer is found to be equal to 1% of the weights of the binder (cement+silica). During the casting of the specimens, three cubes (150 mm on each side) and

Table 3 Proportions of FM mix

Component	Portland cement	Silica fume	Fine aggregate (sand)	Water	Superplasticizers	PP Fiber
Quantity (kg/m ³)	650	65	1310	225	7.15	0.9



Fig. 1 PP fiber used in this work

cylinders (150×300 mm) were taken from the FM mix to gauge the compressive and splitting tensile strengths. After 28 days, FM obtained respective compressive and splitting tensile strengths of 38 and 3.8 MPa.

3.1.2 Reinforcing Steel Bars

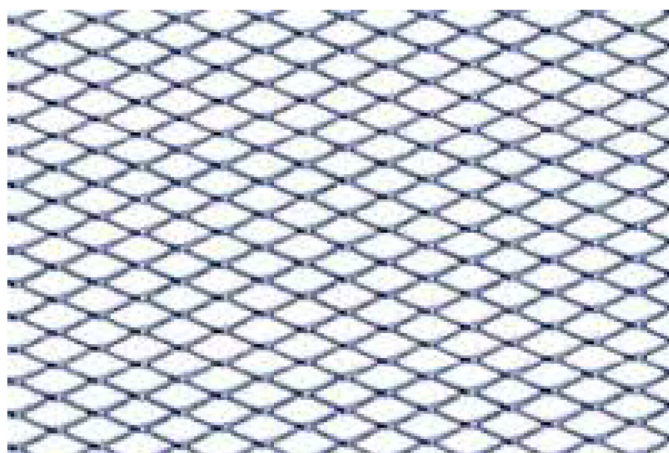
Both the NC and FM specimens used high tensile steel longitudinal reinforcing rebars (HTS). Based on tension tests, the three HTS samples’ average test results revealed that the material’s proof stress and ultimate strength were 551 MPa and 670 MPa, respectively. As shear reinforcement, mild normal steel (NMS) stirrups with diameters of 8 mm and 6 mm were employed for the tested specimens, which had nominal yield stresses of 240 MPa and 350 MPa, respectively.

3.1.3 Reinforcing Steel Meshes

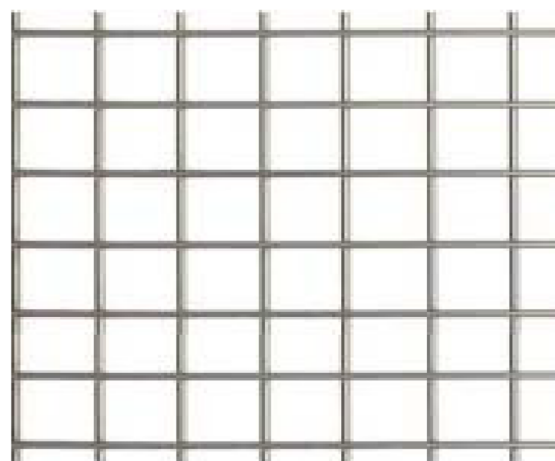
Expanded steel mesh and welded wire mesh were the two types of steel mesh used. A diamond-shaped expanded steel mesh (ESM) was measured 31 mm×16.5 mm and weighed 1.5 kg/m². As seen in Fig. 2a, this kind is constructed using steel sheets with a 1.25 mm thickness that was employed as reinforcing elements. One strand has a cross-sectional area of 1.25 mm×1.25 mm. The mechanical properties of three mesh samples were examined using the Universal Testing Machine. The mesh has an elastic modulus of 120 GPa, an ultimate strength of 350 MPa, and a proof stress of 250 MPa. As seen in Fig. 2b, welded square galvanised steel mesh (WWM) with 12.5×12.5 mm dimensions and 0.45 kg/m² weight was used. The WWM has an elastic modulus of 170 GPa, a proof stress of 400 MPa, and an ultimate strength of 600 MPa.

3.2 Shear Wall Specimens

The experimental program is composed of ten shear walls. All specimens had same size. The cross-section was 150×800 mm and the height was 1500 mm. Ten specimens were divided into two identical groups, V and H. Each group consisted of five specimens. Specimens of group V are subjected to vertical loads whilst specimens of group H are carried by horizontal load. Reinforcement details of each specimen in group H is similar to one specimen in group V, so only details of five specimens will be explained in this section. Group V is composed of one control shear wall made from normal concrete (NC) and four specimens made from ferrocement mortar (FM). All five specimens included an inner hollow 50×700 mm that continued in



(a) Expanded steel mesh ESM



(b) Welded wire mesh WWM

Fig. 2 Steel meshes used

overall height. All five specimens had the same longitudinal reinforcing rebars, which each specimen was reinforced by three 12 mm-HTS bars (3Ø12) positioned at each shorter side as well as two 10 mm-HTS bars (2Ø10) positioned at each longer side (Fig. 3). Longitudinal reinforcement of shear walls was selected to be larger than the minimum limit stated in the Egyptian code (El-Kholy & Dahish, 2016). Table 4 lists details of all five shear walls. Shear reinforcements were either stirrups (Nv, Nh, Fv0 and Fh0) or steel meshes (rest specimens). Stirrups are 8 mm-NMS bar spaced at 200 mm. Specimens Fv,web and Fh,web do not have any shear reinforcement but include one transverse web with 50 mm thickness inside the inner hollow (Fig. 3b). FvE and FhE were provided by two layers of ESM while FvW and FhW were provided by two layers of WWM.

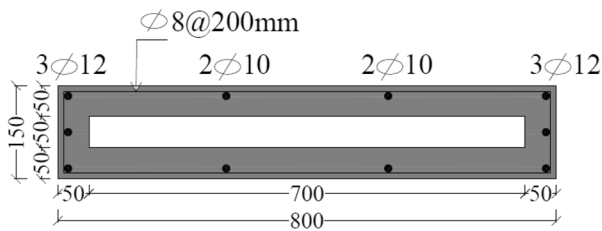
Equations (1) and (2) were used to estimate longitudinal and lateral reinforcement for all specimens. Two solid parts (200 mm thickness) were conducted at the specimen ends to a void local failure due to loading concentration.

$$\mu_l = \frac{A_s}{A_c}, \tag{1}$$

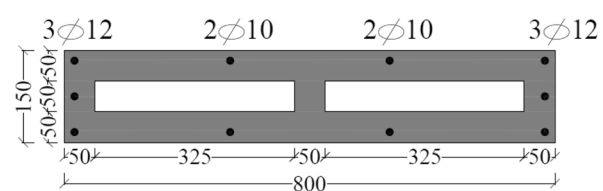
where A_s is the steel area in longitudinal direction and A_c is net area of the cross-section.

$$\mu_t = \frac{V_s}{V_c}, \tag{2}$$

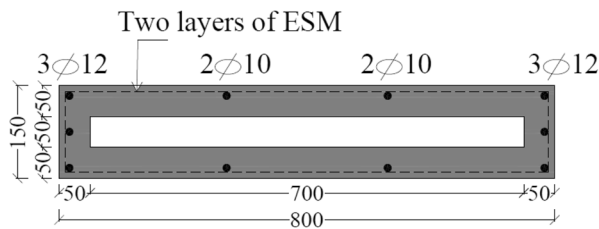
where V_s is the total volume of the shear reinforcement within overall height of the specimen and V_c is the net volume of the specimen.



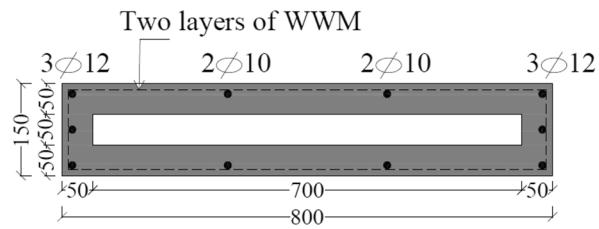
(a) Nv, Nh, Fv0 and Fh0



(b) Fv,web or Fh,web



(c) FvE or FhE



(d) FvW or FhW

Fig. 3 Specimens cross-sections, dimensions in mm

Table 4 Specimens geometry

Specimen ID	Lateral web	Longitudinal bars			Lateral reinforcement		
		Short side	Long side	Ratio μ_l (%)	Stirrups	Steel meshes	Ratio μ_t (%)
Nv or Nh	No	3Ø12	2Ø10	1.17	Ø8@200 mm	No	0.535
Fv0 or Fh0	No	3Ø12	2Ø10	1.17	Ø8@200 mm	No	0.535
Fv,web or Fh,web	With	3Ø12	2Ø10	1.17	No	No	0
FvW or FhW	No	3Ø12	2Ø10	1.17	No	2 layers of WWM	0.27
FvE or FhE	No	3Ø12	2Ø10	1.17	No	2 layers of ESM	0.81

First letter N and F is referred to specimen cased from NC and FM. The second letter v and h denoted to loading type either vertical (v) or horizontal (h). Third letter; 0 means that this specimen was reinforced with conventional stirrups and with no ESM or WWM, web means that inner hole was provided with lateral web, E refers to ESM and W refers to WWM

The specimens were prepared and cast over the course of various stages. Wooden shapes were first created. Second, the use of reinforcement bars was made. Thirdly, the inner hollow was made using low-density foam blocks. Fourth, the necessary ESM and WWM layers were fully encircled around the reinforcing cages. Finally, concrete mixtures made of NC or FM were cast inside the specimens.

3.3 Test Setup and Measurements

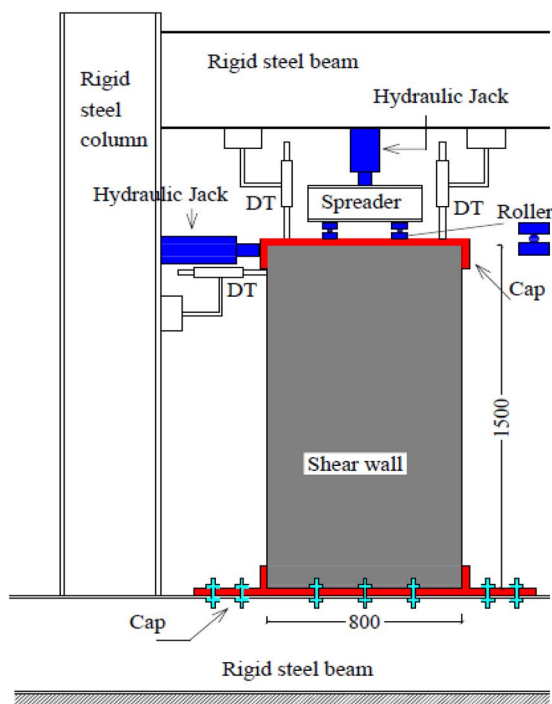
The test setup and instruments are shown in Fig. 4. A hydraulic jack with a 5000 kN capacity provided the vertical load for the tested column's top. Also, a hydraulic jack with a 3000 kN capacity provided the lateral horizontal load for the tested column's top. Load cells were attached to the jacks to record the applied loads during testing. At the two ends of the shear wall, rigid steel caps, with 200 mm depth, were installed to prevent local concrete crushing and well distributed the applied loads. The vertical load was acted on a steel spreader beam. Two roller supports were used between a steel spreader beam and the top cap to allow free horizontal displacement of the specimen. To prevent rotation of the specimen base and serve as a fixed support, the bottom cap was securely fastened to a robust steel beam using bolts. As previously

indicated, group V's five specimens underwent axial loading, while group H's five specimens underwent incremental horizontal loading after being subjected to a constant vertical force of 15% of its ultimate vertical loads. The vertical displacement (shortening) of the specimen was determined using two displacement transducers (DT) positioned vertically on the shear wall crown. Two transducers' average (Δv) was taken into consideration. Additionally, DT was used to measure the horizontal displacement of the specimen's top in the long direction (Δh). To computerize the recording of all data, all DTs and load cells were connected to a data logger. Each specimen of a shear wall also has its crack patterns marked.

4 Results and Discussion

4.1 Load-Sharenting Response

Fig. 5 shows axial load-shortening ($P_v-\Delta v$) curves of group V-specimens. It was seen that the relationships were similar rather. From beginning to around 30% of ultimate load, the linear behavior occurred. After that, specimens exhibited a nonlinear relationship up to the peak. Whenever the load increased from beginning to the peak, the curve slope (stiffness) declined, especially after 60–75% of the peak due to the occurrence of vertical cracks. Once the load reached the peak, the curve



(a) Schematically diagram



(b) Lab photo

Fig. 4 Test setup and instruments

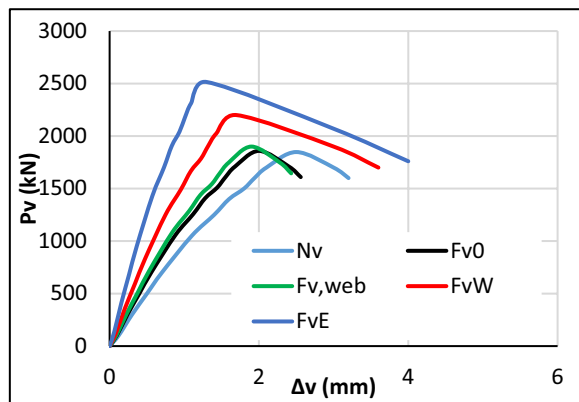


Fig. 5 Vertical load versus shortening (P_v - Δv) relationships

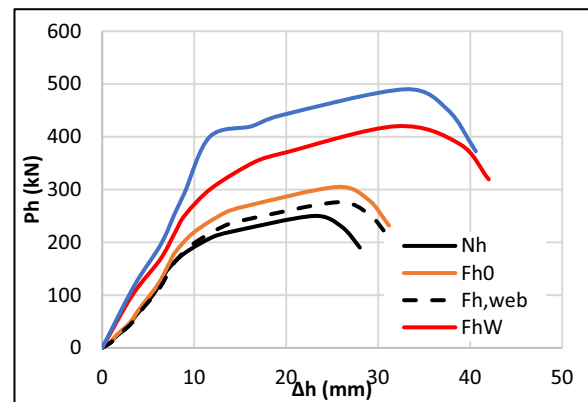


Fig. 6 Lateral load versus horizontal displacement of the shear wall top

quickly dropped. But the decline post peak slightly took place in two shear walls FvW and FvE due to use of steel meshes. The behavior of ferrocement shear wall (Fv0) was slightly better than that of a normal concrete one (Nv) despite the absence of coarse aggregate. Demonstrating the efficiency of ferrocement shear walls compared to normal concrete shear walls. It may be due to the existence of the fibers that may have delayed the occurrence of the vertical cracking. When the lateral stirrups were removed and the transverse web was conducted inside the inner hollow in specimen Fv,web, the behavior nearly identical with specimen Fv0 with stirrups. Demonstrating the big role of transverse web inside inner hollow in preventing lateral distorted of the thin walls of specimens. Also Fig. 5 shows that Fv,web had slightly better performance than Fv0 which could be due to the additional area of concrete due to the presence of the web. It was known that the use of lateral reinforcement caused passive confinement of the concrete core, hence. Its compressive strength increased, hence the shear wall capacity increased. Lateral reinforcement ratio (μ_t) used in specimens Nv, Fv was 0.535% (separated stirrups $\text{Ø}8@200$ mm) while μ_t used in specimens FvW and FvE was 0.27% and 0.81%, respectively, (continued steel meshes within height). Although specimens Nv, Fv had a higher lateral reinforcement ratio more than that of FvW, behavior of FvW was clearly improved better than Nv, Fv due to continuity of steel mesh increased the confinement. Also, the behavior of FvE, with μ_t equal 0.81%, was higher than that of FvW, with μ_t equal 0.27%. Showing that as lateral reinforcement and vertical reinforcement due to the presence of the vertical component of the steel mesh ratios increased, the specimen behavior improved more.

Fig. 6 shows the lateral load-horizontal displacement (P_h - Δh) curves of group H-specimens. These specimens were vertically loaded by 15% of its ultimate vertical

loads before beginning lateral loading. It was seen that the relationships were rather similar. From the beginning to around 60–65% of ultimate load, the linear behavior occurs. Up to this loading level, the cross-section of the shear wall resisted compression stresses at all sides. Once the first crack occurred, the displacement increments clearly increased, causing a horizontal part in the curve. In this stage, the cross-section of the shear wall became subject to tension at one side as well as compression at other side. Due to weakness of concrete tensile strength, a horizontal part took place in the curve. Once the load reached the peak, the curve quickly dropped. The behavior of ferrocement shear wall (Fh0) was better than that of a normal concrete one (Nh) demonstrating of the ferrocement shear walls compared to normal concrete shear walls. The ultimate load and stiffness of Fh0 increased by 22% and 2.5%, respectively, than Nh because adding fibers in FM delayed the occurrence of the cracks and prevented opening and lengthening the crack track. When lateral stirrups were removed and the transverse web was conducted inside inner hollow in specimen Fh,web, the behavior slightly improved compared with specimen Fh0 with stirrups due to continuity of steel mesh increased the confinement. Although specimens Nh, Fh had a higher lateral reinforcement ratio more than that of FhW, the behavior of FhW was clearly improved better than Nh, Fh due to continuity of steel mesh increased the confinement. Also, the behavior of FhE was higher than that of FhW, showing that as lateral reinforcement ratio increased, the specimen behavior improved more.

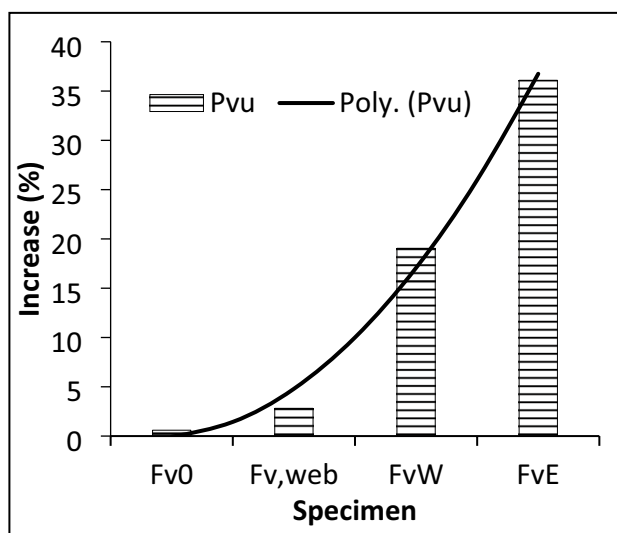
4.2 Ultimate Load

Ultimate vertical load (P_{vu}), ultimate shortening (Δv_u), stiffness (k_v), and energy dissipation capacity (EDC_v) were obtained from P_v - Δv as shown in Fig. 7 and listed in Table 5. Increase ratios in the P_{vu} of all specimens

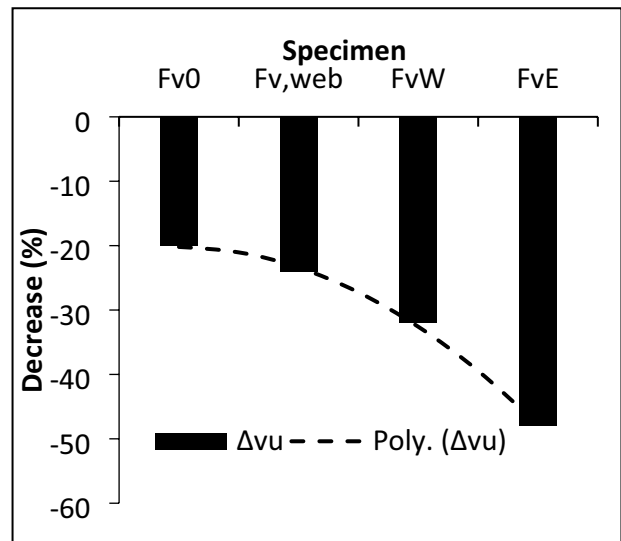
referenced to control specimen (Nv) were calculated (Table 5) and drawn in Fig. 7a. Three specimens, Nv, Fv0 and Fv,web achieved similar Pvu, approximately. These results showed the feasibility of using FM instead of NC to create shear walls. Also, they showed the feasibility of using webs inside a hollow instead of lateral stirrups. Use of WWM (with $\mu_t=0.27\%$) as a lateral reinforcement instead of lateral stirrups (specimen FvW) increased the Pvu by 19% compared to Nv. Additionally, use of ESM (with $\mu_t=0.81\%$) as a lateral reinforcement instead of lateral stirrups (specimen FvE) increased the Pvu by 36.1%

compared to Nv. Showing a combination of FM and steel meshes to create shear walls is considered an excellent alternative to NC shear walls reinforced with separated disconnected stirrups because steel mesh achieved continuity in concrete confinement through whole column height.

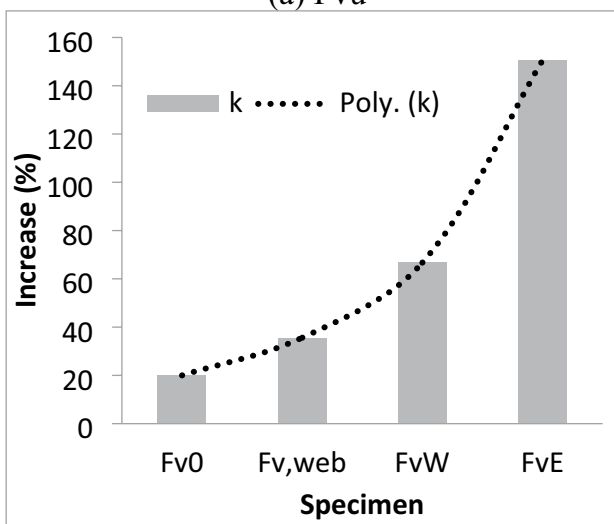
Ultimate horizontal load (Phu), ultimate displacement (Δhu) at the top of the shear wall, stiffness (kh), and energy dissipation capacity (EDCh) were obtained from Ph- Δh shown in Fig. 6 and listed in Table 6. Increase ratios in the Phu of all specimens referenced to control



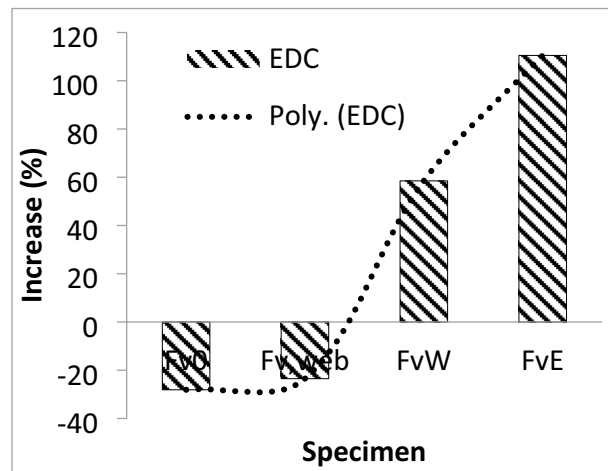
(a) Pvu



(b) Δvu



(c) k



(d) EDC

Fig. 7 Change in performance of axial loaded FM shear walls compared to control NC specimen (Nv)

Table 5 Results of axial loaded shear walls (group V)

Specimen	Pvu (kN)	Increase in Pvu (%)	Δv_u (mm)	Decline in Δv_u (%)	Kv (kN/mm)	Increase in k (%)	EDCv (kN mm)	Change in ECDv (%)
Nv	1848	0.0	2.5	0	1000	0.0	3517	0.0
Fv0	1859	0.6	2	20	1200	20.0	2530	- 28.1
Fv,web	1900	2.8	1.9	24	1356	35.6	2691	- 23.5
FvW	2200	19.0	1.7	32	1667	66.7	5575	58.5
FvE	2515	36.1	1.3	48	2505	150.5	7404	110.5

specimen (Nv) were calculated (Table 6) and drawn in Fig. 8a. As expected, the effect of using FM-steel meshes composite on the Phu was more significant than axial loading because the lateral loading creates tensile stresses acting on the shear walls, especially at high loading levels. The Phu of FM shear wall Fh0 was 22% higher than NC shear wall Nh showing feasibility of using FM instead of NC to create shear walls especially in the case of lateral loading (seismic). The Phu of FM shear wall Fh,web was 10.4% higher than NC shear wall Nh due to the existing web despite the absence of stirrups. Use of WWM (with $\mu_t=0.27\%$) as a lateral reinforcement instead of lateral stirrups (specimen FhW) increased the Phu by 68% compared to Nv. Additionally, use of ESM (with $\mu_t=0.81\%$) as a lateral reinforcement instead of lateral stirrups (specimen FhE) increased the Phu by 96% compared to Nv. Showing a combination of FM and steel meshes to create shear walls is considered an excellent alternative to NC shear walls reinforced with separated disconnected stirrups. For two main reasons; the first is that steel mesh achieved continuity in concrete confinement through whole column height and the second is that the addition of fibers delayed the cracking.

By comparing the results of the two groups V and H, it was found that the methods used in the current study were more effective in the case of horizontal loading than vertical loading. The maximum increase in ultimate vertical load reached 96% in the case of horizontal loading, while the maximum increase reached 36% in the case of vertical loading.

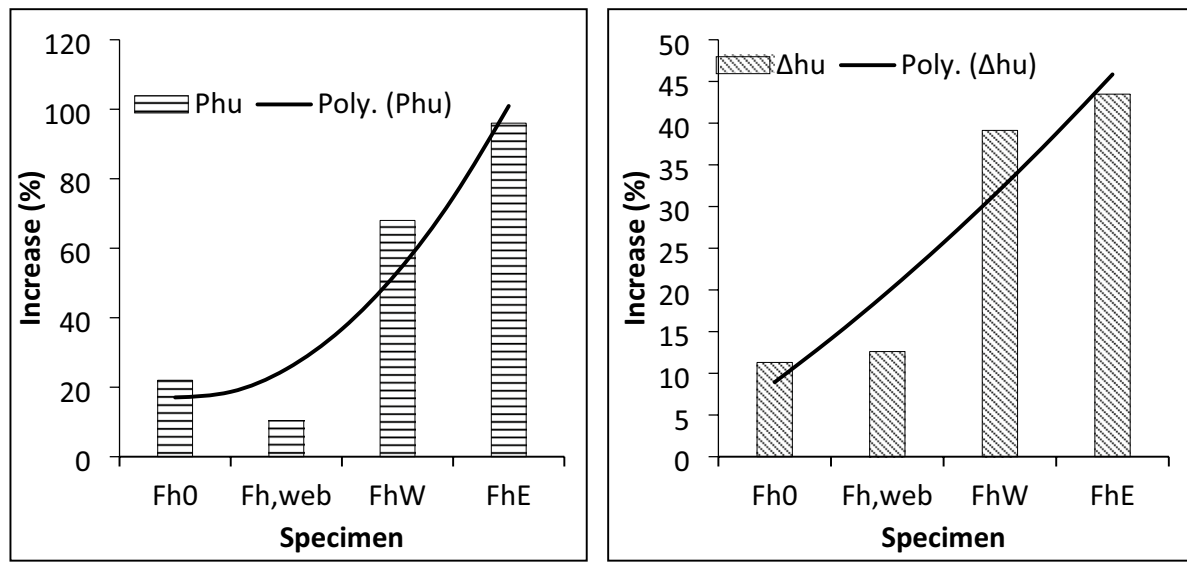
4.3 Ultimate Deformation

After showing the positive effect of the methods used on the maximum load, it is necessary to know the effect on the maximum displacement. At any loading level, it was seen that the vertical (Δv) and horizontal (Δh) displacements of each FM shear wall are less than that of control NC specimen (Nv or Nh), as shown in Figs. 5 and 6. This is an evidence that the deformation of ferrocement mortar is less than normal concrete under the influence of vertical and lateral loads. Results of ultimate vertical (Δv_u) and horizontal (Δh_u) displacements of tested shear walls are listed in Tables 4 and 5, respectively. For specimens of group V that were axially loaded, it was noticed that all FM specimens achieved Δv_u less than that of NC one (Nv), where decline ratios ranged from 20 to 48%. Δv_u of Fv0, Fv,web, FvW and FvE were 20, 24, 32 and 48%, respectively, less than that of Nv (Fig. 8b). Perhaps the reason for this is that the FM mix is less porous and therefore denser, and this leads to a decrease in compressibility compared to NC. Also, the use of fibers reduces strain and restricts compressibility. Moreover, the use of metal meshes (FvW and FvE) prevents accidental straining and leads to shortages of shortening.

For specimens of group H that laterally loaded, it was noticed that all FM specimens achieved Δh_u higher than that of NC one (Nh), where rising ratios ranged from 11.3% to 43.5%. This is the opposite of what happened with the Δv_u that the Nh spacemen achieved Δv_u higher than that of FM specimens. Because the horizontal displacement does not depend on

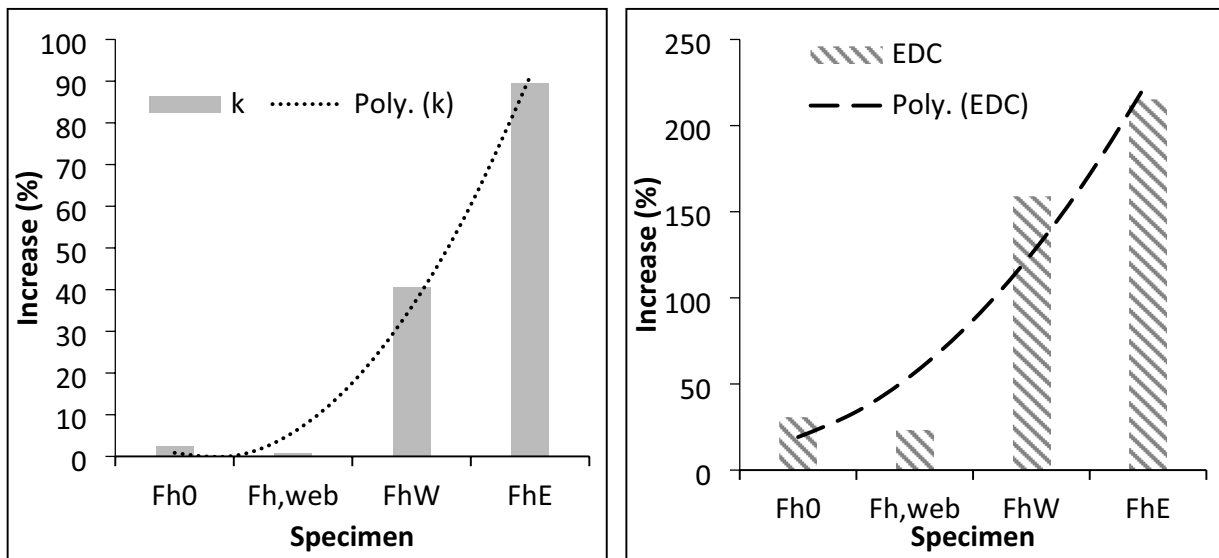
Table 6 Results of lateral loaded shear walls (group H)

Specimen	Phu (kN)	Increase in Phu (%)	Δh_u (mm)	Rise in Δh_u (%)	k (kN/mm)	Increase in k (%)	EDCh (kN mm)	Change in ECDh (%)
Nh	250	0.0	23	0.0	18.05	0.0	4890	0.0
Fh0	305	22.0	25.6	11.3	18.5	2.5	6372	30.3
Fh,web	276	10.4	25.9	12.6	18.2	0.8	6023	23.2
FhW	420	68.0	32	39.1	25.4	40.7	12,655	158.8
FhE	490	96.0	33	43.5	34.2	89.5	15,390	214.7



(a) Phu

(b) Δhu



(c) k

(d) EDC

Fig. 8 Change in performance of lateral loaded FM shear walls compared to control NC specimen (Nh)

compressibility in the concrete, but it depends on the bending capacity of the shear wall. It is worth noting that the shear wall section bears compression and tension together. Therefore, it is expected that the stronger a specimen, the greater the horizontal displacement. Δh_u of Fh0, Fh,web, FhW and FhE were 11.3, 12.6, 39.1 and 43.5%, respectively, bigger than that of Nh

(Fig. 9b). Perhaps the reason for this is that the FM mix is less porous and therefore denser, and this leads to an increase in capacity compared to NC. Also, the use of fibers increases the capacity. Moreover, the use of metal meshes (FhW and FhE) prevents accidental straining and leads to increase in confinement and leads to a rise of the capacity.

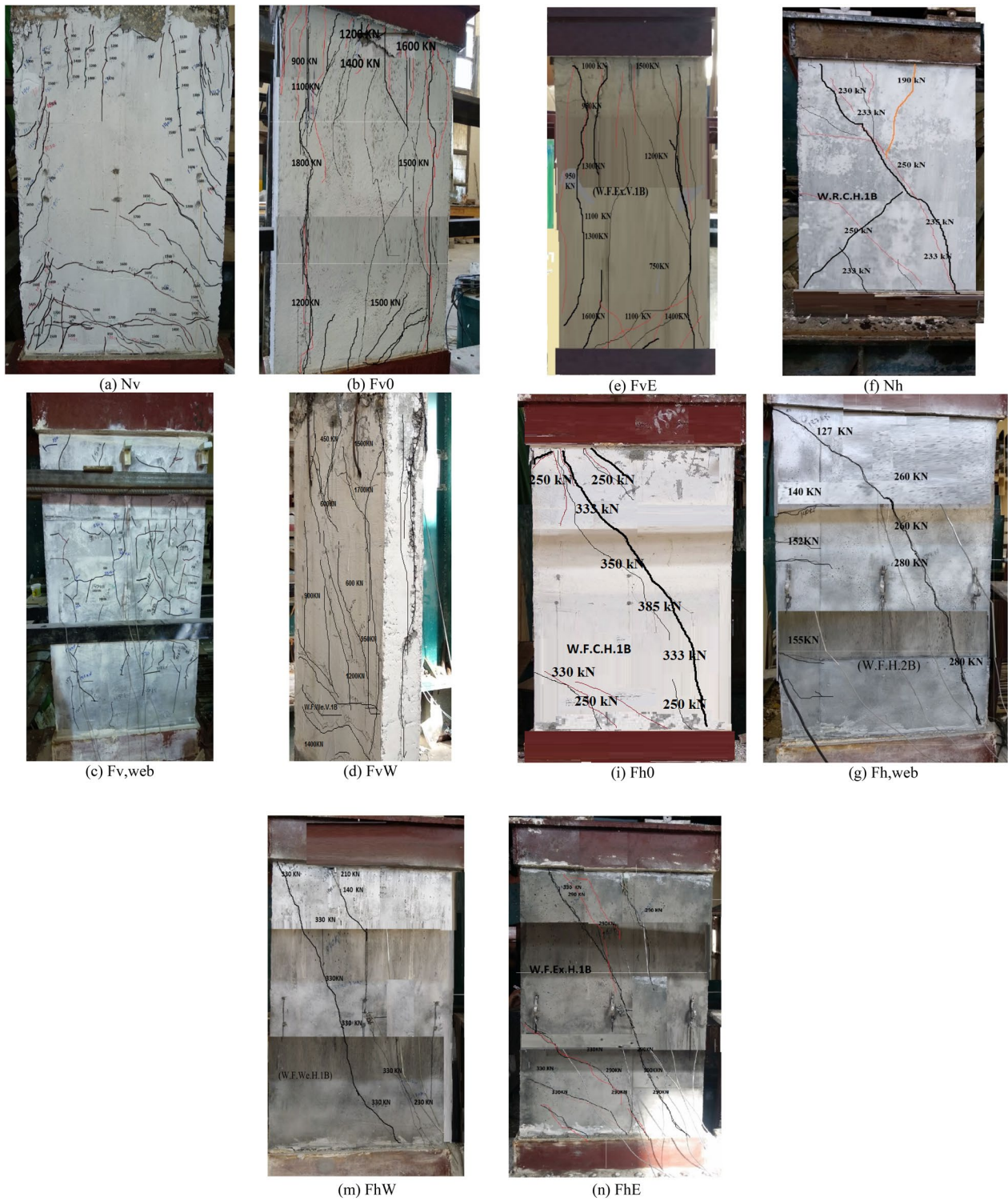


Fig. 9 Failure modes of shear walls

4.4 Stiffness

Stiffness is the extent to which an object resists deformation in response to an applied force. Stiffness is

defined as the resistance to a force causing a member to bend. Stiffness and strength of shear walls are the most important characteristics for evaluation analysis of the

structural behavior. After showing the effect of the methods used on the ultimate load and deformations, it is necessary to understand stiffness behavior of FM shear walls compared to NC one. In this study, stiffness of each specimen was estimated by slope of the linear part at beginning the load–displacement curve. Values of vertical (kv) and horizontal (kh) stiffness of tested shear walls of group V and H are listed in Tables 5 and 6, respectively. For both specimens that were axially and laterally loaded, it was shown that vertical (kv) and horizontal (kh) stiffness of FM were higher than those of NC specimens (Nv and Nh). Where increase ratios ranged from 20 to 150.5% in group V and it ranged from 2.5 to 89.5% in group H. For specimens of group V that axially loaded, kv of Fv0, Fv,web, FvW and FvE were 20, 35.6, 66.7 and 150.5%, respectively, higher than that of Nv (Fig. 7c). Not only the FM walls achieved an increase in the maximum load, but also they achieved an increase in the stiffness. FvE was reinforced with the highest ratio of lateral reinforcement ($\mu_t=0.81\%$) so it achieved the largest increase (150.5%) compared to all specimens.

Despite the large increasing percentage of stiffness (kv) that occurred with axially loaded walls, it is important to know the increasing percentages of stiffness (kh) that occurred with laterally loaded, because the walls mainly resist earthquakes not gravity loads. For specimens of group H that axially loaded, kh of Fh0, Fh,web, FhW and FhE were 2.5, 0.8, 40.7 and 89.5%, respectively, higher than that of Nh (Fig. 8c). It was seen that effect of using FM instead of NC had an unnoticeable role on horizontal stiffness (kh). Also, the web inside the inner hollow had an unnoticeable role in the kh. In contrast, using two layers of WWM in specimen FvW enhanced the kh by 40.7% compared to Nh. Additionally, FhE was reinforced with the highest ratio of lateral reinforcement ($\mu_t=0.81\%$ and two layers of ESM) so it achieved a largest increase (89.5%) compared to Nh.

4.5 Energy Dissipation Capacity

The ductility is an indication of the plastic deformation amplitude in the tested specimens. Two strategies were implemented to compute the column ductility coefficient examined in Emara et al. (2021). The first strategy (ductility index) depends on the vertical displacement, so it was computed by the ratio between both vertical displacement at yielding and the maximum displacement (Emara et al., 2021; Walid & Fayed, 2021). The second strategy (energy dissipation capacity, EDC) is the total area under the $P-\Delta$ curve (Hadi, 2006, 2007). In this study, EDC calculated for all the tested walls is listed in Tables 5 and 6 for group V and H, respectively. The ductility index was not calculated as the laterally loaded walls failed due to

the diagonal tensile crack (shear failure) before yielding of longitudinal bars.

Fig. 7d shows change in EDCv of specimens of group V. It was noticed that energy dissipation capacity (EDCv) of two specimens, Fv0 and Fv,web was slightly declined compared to that of NC wall (Nv). Use of two layers of WWM increased EDCv of FvW by 58.5% compared to that of NC wall (Nv). While using two layers of ESM increased EDCv of FvE by 110.5% compared to that of Nv. Based on results of EDCv, to achieve an increase in the capacity, stiffness and ductility of the walls, it is not necessary to use FM reinforced with steel meshes. Because the task of shear walls is to resist earthquakes, it is important to know the ductility of group H. Fig. 8 shows changes in EDCh of laterally loaded FM shear walls compared to control NC specimen (Nh). It was found that the EDCh of all FM walls was significantly enhanced with respect to NC wall (Nh). The EDCh of Fh0, Fh,web, FhW and FhE were 30.3, 23.2, 158.8 and 214.7%, respectively, higher than that of Nh. So, use of FM, transverse web, two layers of WWM and two layers of ESM had a significant effect on the EDCh. Therefore, it is recommended that the methods used in this work are effective in resisting earthquakes.

4.6 Failure Modes

In Fig. 9, the cracking pattern of the tested walls is depicted. For group V, the first cracks appeared near the side of the specimens. The load increased, causing the fissures to spread vertically and produce new cracks. The cracks began to spread diagonally as the specimen neared its failure load. The modes of failure for all specimens of group V are compression failure and they accompanied with local spalling and crushing of the concrete cover for the Nv and Fv0. On the faces of the walls, a significant vertical crack formed upon failure. Compared to FM walls, the NC wall had fewer formed cracks. Although the crack width for two walls, FvW and FvE was not measured, it was noted that the dispersion of the steel wire reinforcement was the cause of the wide cracks. The failure of the specimens occurred in the laterally loaded walls of group H (Fig. 9f–n) due to reaching the ultimate shear stresses, and a substantial diagonal shear crack developed and contributed to the failure due to the hollow core's weak shear resistance. The modes of failure for all specimens of group h are flexural-shear cracks.

5 Conclusion

Ten shear walls were tested in this article; five of them under axial compressive load and five under lateral load. Eight walls were constructed using ferrocement mortar (FM), while two controls were constructed using normal concrete (NC). The wall was 150 mm wide, 800

mm thick, and 1500 mm in height. A 50×700 mm inner longitudinal hole that went through the wall height was made. While transverse reinforcement varied in type and ratio, longitudinal reinforcement used high tensile bars with a constant ratio of 1.17% for all ten walls. Traditional stirrups were used to lateral reinforce two control NC walls and two FM walls with a ratio of 0.535%. Two layers of welded wire mesh (WWM) with a ratio of 0.27% were used to lateral reinforce two FM walls. With a ratio of 0.81%, two layers of expanded steel mesh (ESM) were used to lateral reinforce two FM walls. Two remaining specimens had one transverse web in the middle of the inner hole but were otherwise free of lateral reinforcement. Walls were separated into two symmetric groups (V and H), each of which contained five walls. Group V was loaded axially, whilst group H was loaded laterally. In group V, it was looked into how FM walls compared to NC walls in terms of their load-shortening response, ultimate axial load and corresponding ultimate shortening, stiffness, ductility, and failure mechanism. Investigated in group H were the stiffness, ductility, and failure mode of FM walls in comparison to NC walls, as well as the load-lateral drift response, ultimate lateral load, and corresponding ultimate drift. According to the findings, the following observations can be made:

- (1) Load–displacement relationship, ultimate axial load and corresponding ultimate shortening of FM walls, with stirrups and with web instead of stirrups, slightly improved (maximum change ratio 24%) more than control NC wall in two loading systems (axial and lateral). Use of WWM/ESM significantly improved load–displacement relationships of FM walls more than control NC wall in two loading systems.
- (2) FM walls reinforced with WWM and ESM had ultimate axial loads that were, respectively, 19% and 36%, higher and related ultimate shortenings that were, respectively, 32% and 48%, lower than control NC walls.
- (3) FM walls reinforced with WWM and ESM had ultimate lateral loads and related ultimate drift that were, respectively, 68% and 39%, 96% and 43.5%, higher than control NC wall.
- (4) Increase ratios in the stiffness of FM walls ranged from 2.5% to 89.5% in the case of lateral loading, more than the control NC wall and from 20% to 150.5% in the case of axial loading.
- (5) As two layers of WWM were used to laterally reinforce FM walls, the ductility increased when compared to NC walls by 58.5% and 158.8% for axial and lateral loading, respectively. In comparison to NC wall, the application of two layers of ESM to

laterally reinforce FM walls increased their ductility by 110.5% and 214.7%, respectively, under axial and lateral loads.

- (6) Lateral reinforcement and vertical reinforcement due to the presence of the vertical component of the steel mesh ratios increased, and the specimen's behavior improved more.

Acknowledgements

The tests were carried out in the concrete laboratory, Faculty of Engineering, Tanta University, Egypt.

Author contributions

Boshra A. Eltaly and Youssry B. Shaheen: Resources, Investigation, Data curation, Reviewing, Samar Khiry: Investigation, Data curation, Validation, Visualization, Writing—review & editing. Sabry Fayed: Investigation, Data curation, Writing—original draft, Visualization.

Funding

Open access funding provided by The Science, Technology & Innovation Funding Authority (STDF) in cooperation with The Egyptian Knowledge Bank (EKB).

Declarations

Competing interests

The author declares that there are no known conflicts of interest related to this publication and that no substantial financial support has been provided for this work that would have affected its conclusion.

Received: 8 December 2022 Accepted: 31 March 2024

Published online: 04 July 2024

References

- ACI 549.1R-93 & ACI 549-1R-88, A. C. I. Guide for the Design Construction, and Repair of Ferrocement, ACI Committee 549.1R-93; ACI 549-1R-88 and 1R-93, (1997).
- ACI 549R-97, State-of-the-Art Report on Ferrocement, American Concrete Institute, Detroit, MI 48219 (1993), USA
- ACI Committee 549 State-of-the-Art report on ferrocement. ACI549-R97, in manual of concrete practice. ACI, (1997) Detroit, p. 26.
- Altheeb, A. H. (2016). *Seismic drift capacity of lightly reinforced concrete shear walls*. Diss. University of Melbourne.
- Christidis, K. I., & Karagiannaki, D. (2021). Evaluation of flexural and shear deformations in medium rise RC shear walls. *Journal of Building Engineering*, 42, 102470.
- Christidis, K. I., & Trezos, K. G. (2017). Experimental investigation of existing non-conforming RC shear walls. *Engineering Structures*, 140, 26–38.
- Data sheet of Sika VisCocrete 3425. (2024). <https://egy.sika.com/content/dam/dms/eg01/e/Sika%20ViscoCrete%C2%AE%20-3425.pdf>.
- El-Kholy, A. M., & Dahish, H. A. (2016). Improved confinement of reinforced concrete columns. *Ain Shams Engineering Journal*, 7(2), 717–728.
- Eltehawy, E. (2009). Effect of using ferrocement on the mechanical properties of Reinforced Concrete Slabs subjected to Dynamic Loads. in *13th international conference on aerospace science and aviation technology (ASAT)*
- Emara, M., et al. (2021). Behavior of ECC columns confined using steel wire mesh under axial loading. *Journal of Building Engineering*, 43, 102809.
- Gaba, H., & Harvinder, S. (2008). The Study of Economy of Ferrocement with Fly Ash as an Admixture. in *12th international conference of international association for computer methods and advances in geomechanics*
- Ganesan, N., Indira, P. V., & Thadathil, S. P. (2011). Effect of ferrocement wrapping system on strength and behavior of RC frames under reversed lateral cyclic loading. *Experimental Techniques*, 35(4), 23–28.

- Greepala, V., & Nimityongskul, P. (2006). Structural integrity and insulation property of ferrocement exposed to fire. *Journal of Ferrocement*, 36(4), 939.
- Greifenhagen, C., & Lestuzzi, P. (2005). Static cyclic tests on lightly reinforced concrete shear walls. *Engineering Structures*, 27(11), 1703–1712.
- Hadi, M. N. S. (2007). Behaviour of FRP strengthened concrete columns under eccentric compression loading. *Composite Structures*, 77(1), 92–96.
- Hadi, S. (2006). Behaviour of FRP wrapped normal strength concrete columns under eccentric loading. *Composite Structures*, 72, 503–511.
- Hube, M. A., et al. (2014). Seismic behavior of slender reinforced concrete walls. *Engineering Structures*, 80, 377–388.
- Kaish, A. B. M., et al. (2013). Ferrocement jacketing for restrengthening of square reinforced concrete column under concentric compressive load. *Procedia Engineering*, 54, 720–728.
- Kaushik, S. K., & Singh, S. P. (1999). Behavior of ferrocement composite columns in compression. *Special Publication*, 172, 669–682.
- Kondraivendhan, B., & Pradhan, B. (2009). Effect of ferrocement confinement on behavior of concrete. *Construction and Building Materials*, 23(3), 1218–1222.
- Li, X., et al. (2018). Eccentric compressive behavior of reinforced concrete columns strengthened using steel mesh reinforced resin concrete. *Applied Sciences*, 8(10), 1827.
- Lu, Y., et al. (2017). Cyclic testing of reinforced concrete walls with distributed minimum vertical reinforcement. *Journal of Structural Engineering*, 143(5), 04016225.
- Mansur, M. A., & Paramasivam, P. (1990). Ferrocement short columns under axial and eccentric compression. *Structural Journal*, 87(5), 523–529.
- Motter, C. J., Abdullah, S. A., & Wallace, J. W. (2018). Reinforced concrete structural walls without special boundary elements. *ACI Structural Journal*, 115(3), 723–733.
- Naaman, A. E. (2000). *Ferrocement and laminated cementitious composites* (Vol. 3000). Techno Press.
- Oh, Y.-H., Sang, W. H., & Li-Hyung, L. (2002). Effect of boundary element details on the seismic deformation capacity of structural walls. *Earthquake Engineering and Structural Dynamics*, 31(8), 1583–1602.
- Orakcal, K., Massone, L. M., & Wallace, J. W. (2009). Shear strength of lightly reinforced wall piers and spandrels. *ACI Structural Journal*, 106(4), 455.
- Ravichandran, K., & Jeyasehar, C. (2012). Seismic retrofitting of exterior beam column joint using ferrocement. *International Journal of Engineering and Applied Sciences*, 4(2), 35–58.
- Sasiekalaa, K., & Malathy, R. (2012). A review report on mechanical properties of ferrocement with cementitious materials. *International journal of Engineering Research technology* 11.
- Shaheen, Y. B. I., Mahmoud, A. M., & Refat, H. M. (2016). Structural performance of ribbed ferrocement plates reinforced with composite materials. *Structural Engineering and Mechanics*, 60(4), 567–594.
- Shaheen, Y., Mahmoud, M., & Refat, H. (2017). Experimental and FE simulations of ferrocement columns incorporating composite materials. *Structural Engineering and Mechanics*, 64(2), 155–171.
- Soman, M., & Mohan, J. (2018). Rehabilitation of RC columns using ferrocement jacketing. *Construction and Building Materials*, 181, 156–162.
- Wafa, M. A., & Fukuzawa, K. (2010). Characteristics of ferrocement thin composite elements using various reinforcement meshes in flexure. *Journal of Reinforced Plastics and Composites*, 29(23), 3530–3539.
- Walid, M., & Fayed, S. (2021). Flexural rigidity and ductility of RC beams reinforced with steel and recycled plastic fibers. *Steel and Composite Structures*, 41(3), 317–334.
- Wang, S., Naaman, A. E., & Li, V. C. (2004). Bending response of hybrid ferrocement plates with meshes and fibers. *J Ferrocem*, 34(1), 275–288.
- Xiong, G. J., et al. (2011). Load carrying capacity and ductility of circular concrete columns confined by ferrocement including steel bars. *Construction and Building Materials*, 25(5), 2263–2268.

Publisher's Note

Springer Nature remains neutral with regard to jurisdictional claims in published maps and institutional affiliations.

Yousry B. Shaheen is a Professor in Department of civil engineering, Menoufia University, Shebin El Koum, Egypt

Boshra A. Eltaly is a Professor in Department of civil engineering, Higher Institute of Engineering and Technology, Kafr El sheikh, Egypt

Samar Khairy is an Assistant Professor in Department of civil engineering, Higher Institute of Engineering and Technology, Kafr El sheikh, Egypt

Sabry Fayed is an Associate Professor in Department of civil engineering, Faculty of Engineering, Kafr El-Sheikh University, Kafr El-Sheikh, Egypt,